

DETECTING INVASIVE SERICEA LESPEDEZA (*Lespedeza cuneata*) IN MISSOURI PASTURELANDS WITH HYPER- AND MULTI-SPECTRAL AERIAL PHOTOS

Cuizhen Wang

Assistant Professor, Dept. of Geography, University of Missouri
8 Stewart Hall, Columbia, MO 65211, USA

E-mail: wangcu@missouri.edu

ABSTRACT

Missouri ranks second in cow-calf numbers in the United States and its pastureland has experienced invasion of various plant species. As one of the invasive weeds, sericea is becoming a serious threat to pasturelands in this state. This study used an airborne hyperspectral (AISA) image to map sericea and its invasiveness in a public grass field and a private hayfield in Mid-Missouri. The maximal 1st-order derivative in red-near infrared region was derived to separate sericea from fescue, the dominant grass in the fields. The 2-m multi-spectral aerial photos from the National Agriculture Image Program (NAIP) were also examined to test information loss when data was reduced from narrowband hyperspectral image to broadband aerial photos. The quantitative distribution of sericea in this study could serve as a first step in alerting landowners and the general public about the seriousness of sericea invasion in pasturelands in Missouri.

INTRODUCTION

Weed invasion is a current threat to productivity in croplands and biodiversity conservation in natural ecosystems. Sericea lespedeza (*Lespedeza cuneata* L.), hereafter referred to as sericea, is one type of invasive weed which is becoming a serious threat to cattle production in pastures and uncultivated public lands in Missouri. Sericea is a warm-season, perennial legume native to eastern Asia. In the 1930s, it was introduced into Missouri to control erosion on roadsides and strip-mined lands (Brush 2001). Although sericea cannot survive in highly maintained crop fields that are plowed and harvested periodically, it slowly invades into less-managed pastures and grass lands. Cattle like to graze its young, tender sprouts, but not the more mature stems in which tannin levels are significantly increased (Stitt 1943). The next spring the woody stems protect the tender shoots from cattle grazing which results in denser vegetative growth and dominating patches of sericea. Because of its highly competitive nature, poor forage quality, and strong invasiveness, sericea has been put on the noxious weed list in several states such as Kansas (Dudley and Fick 2003). Although not listed as noxious in Missouri, it has been observed in every county and has been recognized as a “silent thief” in this state (Bové 2004).

In-situ field surveys to regularly document the size, shape, and location of weed populations is time consuming and not economically feasible. Remote sensing is a useful tool to efficiently survey large areas of private and public lands. Typical high-resolution multispectral remote sensing (e.g., aerial photos) has shown promise in detecting agronomic pests such as disease and mites, and late-season weed infestation (Fitzgerald et al. 2004; Koger et al. 2003). However, in pasturelands, the height and greenness of sericea are very similar to those of grass. Due to limited spectral coverage, the broadband spectral signatures typically captured in multispectral images are not capable of discriminating sericea from dominant grass.

Imaging spectrometers, or “hyperspectral sensors”, are remote sensing instruments that combine the spatial presentation of an imaging sensor with the analytical capabilities of a spectrometer (Goetz et al. 1985). Hyperspectral sensors record dozens to hundreds of narrow bands in the visible – infrared spectral region, forming continuous spectral curves which can distinguish the subtle spectral differences of vegetative species (Jensen 2000; Fitzgerald et al. 2004). Past studies have shown that narrowband imagery could improve the capability of detecting vegetation species using optimized spectra-based classification methods such as the spectral angular mapping (SAM) and the spectral mixture analysis (SMA) (Zhang et al. 2003; Fitzgerald et al. 2004). Narrowband vegetation indices have also been modified from typical broadband concepts to detect photosynthetic efficiency (Gamon et al. 1992), nitrogen and water stress (Peñuelas et al. 1994), and diseases and pests in crops (Filella et al. 1995). These studies adopted the concept from broadband remote sensing that each spectral band was an independent variable. Algorithms based on this assumption thus reduced the unique advantage of hyperspectral remote sensing (Tsai and Philpot 1998).

Derivative analysis treats hyperspectral imagery as truly spectrally continuous data. Originally developed in spectroscopy, derivative spectral analysis have been found very useful in remote sensing because it is relatively insensitive to variations in illumination intensity caused by changes in sun angle, cloud cover, or topography (Demetriades-Shah et al. 1990; Peñuelas et al. 1994; Tsai and Philpot 1998). Becker et al. (2005) used 2nd-order derivative analysis to identify optimal spectral bands to classify dominant vegetation classes in coastal wetlands. Some studies have also been conducted to evaluate water quality by estimating concentration of water constituent and suspended sediment (Chen and Curran 1992). Although not many derivative analysis studies have been documented in weed science, the same technique could be applied to maximize local spectral variation between weeds and natural vegetation.

This study used both hand-held spectroradiometer and airborne hyperspectral imagery to map sericea and to quantify its invasiveness in pastures in Mid-Missouri. A 1st-order derivative analysis was applied to calculate maximal derivatives that maximized the spectral difference between sericea and fescue, the dominant grass in pastures. Regular classification methods were also applied to broadband true-color and false-color aerial photos in the study area. Finally, the accuracies of sericea mapping with narrowband and broadband imagery were evaluated.

MATERIALS AND METHODS

Study Area and Data Set

Two fields were selected in this study: a public grass field and a private hay field in Mid-Missouri. The 157-acre public field was the property of the Cedar Creek Ranger District, Mark Twin National Forest. It was minimally managed that served as pasture in the summer and was mowed once per year when grazing was over. The private hay field was managed more actively and was mowed several times per year for forage production. The major vegetation species in these two fields was tall fescue (*Festuca arundinacea*), hereafter referred to as fescue, a common type of grass adapted to the clay soils that dominated Missouri. Sericea was introduced into these lands as soil erosion control a few decades ago. Its invasion into the lands has become apparent and sericea patches of various sizes could be observed all over the study areas.

In summer 2006, state-wide true-color aerial photos (at 2-meter resolution) were collected in Missouri under the National Agriculture Imagery Program (NAIP). In the photo over the public field (Figure 1A), the fescue-dominated grass field was in yellowish tan because it senesced in the hot and dry summer in Missouri. Sericea patches in light green can be observed all over the field. However, their boundaries were often ambiguous in the photo. It was also difficult to identify small sericea patches in this true-color photo. Forests and bare surfaces that were not associated with pastures can be easily discriminated in the NAIP photo. With a standard unsupervised classification, forests and roads around the grass field, as well as ponds and bare soil inside the field, were mapped and masked out in this study.

A hyperspectral image of the public field was acquired on July 19th, 2006 by the Center for Advanced Land Management Information Techniques (CALMIT), University of Nebraska, using the Airborne Imaging Spectroradiometer for Applications (AISA). The AISA image was composed of 63 bands in the spectral range of 430-970 nm (visible - near infrared). The spectral resolution was approximately 10 nm per band. At an instantaneous field-of-view of 0.062°, the spatial resolution of the image was about 1 meter at flight height of 1,000 meters above ground level. In the false-color AISA image (Figure 1B), sericea patches of various sizes showed up in bright red and could be easily differentiated from fescue that was light pink to bluish gray. The image delivered from CALMAT had been radiometrically calibrated and atmospherically corrected with Fast Line-of-sight Atmospheric Analysis of Spectral Hypercubes (FLAASH) algorithm in the ENVI software (ENVI, 1999). The AISA image was not acquired in the private field.

A total of 58 sample sites were selected in two fields, among which 39 sites (27 for sericea and 12 for fescue) were in the public field and 19 sites (11 for sericea and 8 for fescue) were in the private field. In the public field, each sericea site was a relatively homogeneous polygon larger than 3×3 meters so that it could be identified in the AISA image. The fescue sites in similar size were a few meters away from sericea sites. Sericea grew in a clustered pattern and was often mixed with fescue along the edges. Among the 27 sericea sample sites in the public field, eighteen (18) were pure sericea sites and nine (9) were mixed sites in which both sericea and fescue were observed. Most sericea sites in the private field were mixed because sericea could not grow into large patches in more actively managed lands.

On June 15, July 05, August 02, and August 24, 2006, field spectra of sericea and fescue in both fields were repetitively collected at the center of each sample site using the hand-held FieldSpecFR spectroradiometer from

Analytical Spectral Devices (ASD), Inc. The 18° field-of-view fore-optic of the ASD instrument was held in a nadir view at 1.5m above the center of each sample site, providing a circular ground sample of about 0.5m diameter. The FieldSpecFR recorded spectral reflectance of each sample between 350nm-2500nm at an interval of 1nm. The ASD spectra were smoothed with a Savitzky Golay filter to reduce system noises. The filter performed a local polynomial regression to determine the smoothed value for each data point in the ASD spectrum (Savitzky and Golay 1964). The reflectance in 1300-1450nm and 1750-2400nm was highly affected by water vapor absorption and was thus not analyzed in this study. The smoothed ASD spectra were resampled to the same band widths as the AISA image using a Full Width at Half Maximum (FWHF) Gaussian model in the Spectral Library Resampling Tool in the ENVI software (ENVI 1999).

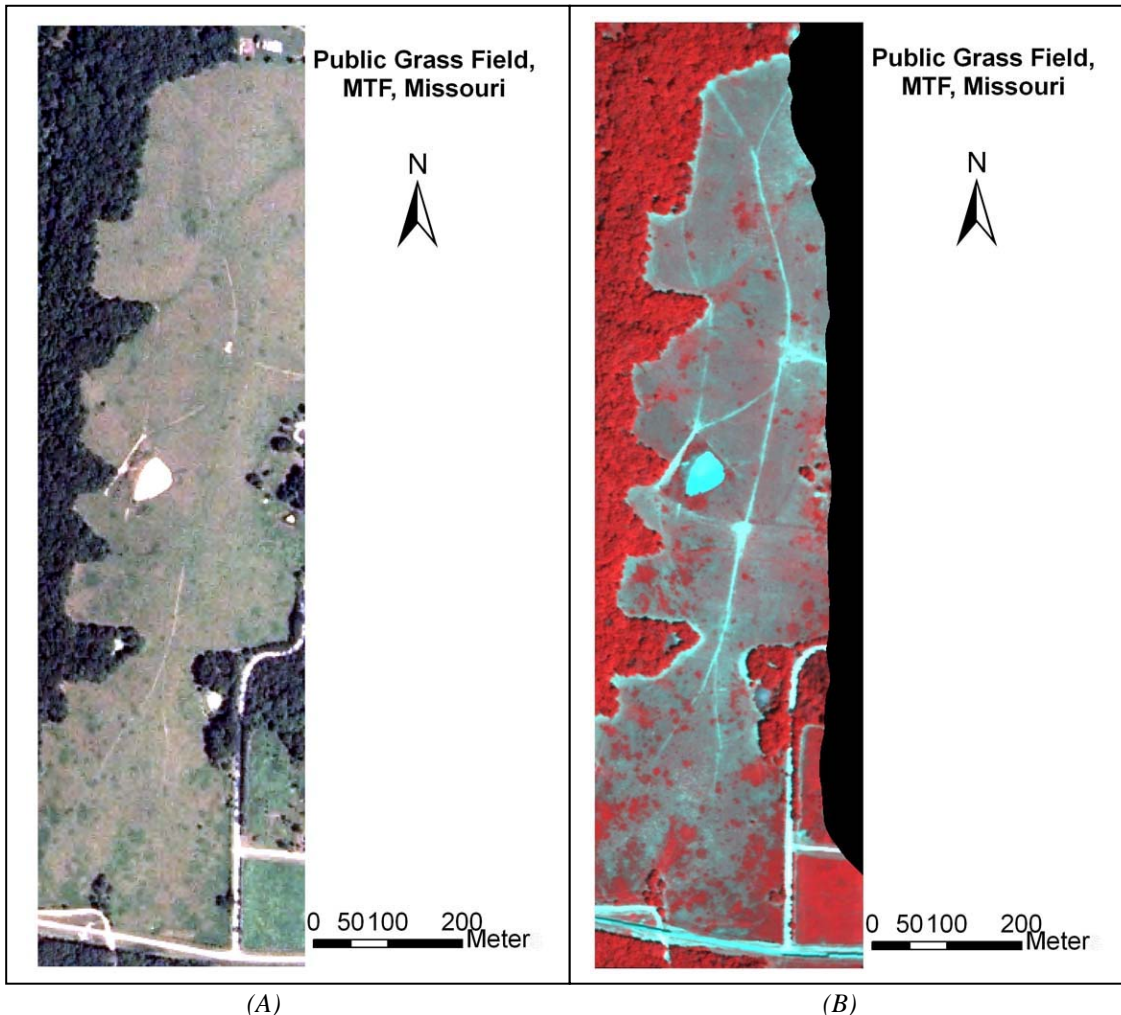


Figure 1. The true-color NAIP aerial photo (A) and the AISA image in false-color display (800nm, 676nm, 657nm as R, G, B) (B) in the public grass field.

During field spectra collection, the average height of sericea at each sample site was measured. A nadir-view digital picture was also taken at 1.5m above the center of each site. When taking pictures, a 3-ft yard stick was laid on the ground to serve as a scale reference. The picture was later cropped into a 0.5m-diameter circle to match the view of the FieldSpecFR. A 30-cluster unsupervised classification (ISODATA) was then performed to the cropped pictures of pure and mixed sericea sites to calculate its ground cover. The yard stick in the pictures was masked out prior to any calculation.

1st-order Derivative Analysis

The reflectance curvatures in the ASD spectra of sericea (Figure 2A) and fescue (Figure 2B) were similar in visible-infrared (NIR) region. Although the average NIR reflectance of sericea was higher than that of fescue, a wide

overlap could be observed in two figures. Mixed sericea also had lower NIR reflectance and higher red reflectance than pure patches with the curves laid between those of pure sericea and rescue. As a result, a typical classification scheme with broadband spectra cannot effectively separate sericea from fescue.

Controlled by biophysical properties of both vegetative species, a higher NIR reflectance was always associated with a lower red reflectance in the spectra. Therefore, the variation of reflectance in the red-NIR region could be explained by the slopes of reflectance curves in this region. The slopes can be measured with a 1st-order derivative that was expressed as (Becker et al. 2005):

$$d^{1st} = (\rho_{n+1} - \rho_n) / (\lambda_{n+1} - \lambda_n) \quad (1)$$

where n is band number, ρ_n is surface reflectance at band n , and λ_n is the wavelength (nm) of this band.

The ASD-measured spectra were averaged over sample sites of sericea and fescue, respectively. The maximal derivatives of both species were located in the range of 650-800nm (the so-called red edge). Since sericea reflected more NIR energy than fescue did, the maximal derivative of sericea was much higher than that of fescue in this region. The derivatives in other spectral regions were similar for these two species.

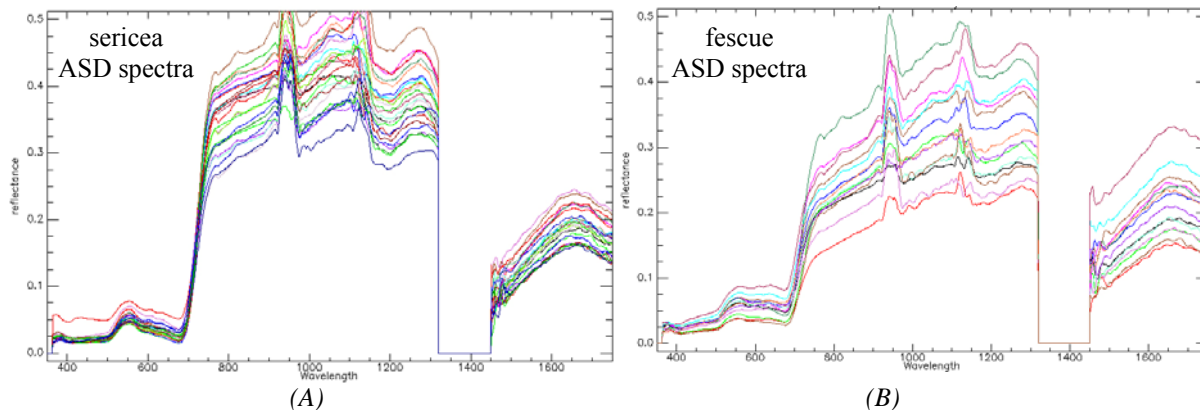


Figure 2. The field spectra of sericea (A) and fescue (B) measured by the ASD FieldSpecFR at sample sites in the public field on August 02, 2006.

The reflectance values at all sample sites in the AISA image were extracted and the maximal derivatives in the 650-800nm spectral range at these sites were calculated. Since a normalization factor of 10,000 was applied to the digital number (DN) at each pixel of the AISA image, the derivatives discussed in the following processes were 10,000 times higher than real derivatives calculated from field ASD spectra. It was found that maximal derivatives in the 650-800nm range enhanced the spectral difference between sericea and fescue. With a threshold of maximal derivative = 40, these two species could be separated:

Maximal derivative > 40 → sericea

Maximal derivative ≤ 40 → fescue

The maximal derivative for each pixel in the hyperspectral AISA image was calculated (in the 650-800nm spectral range). Each pixel was then assigned sericea or non-sericea with this threshold method. Sericea patches in the study area were thus detected from a binary map.

Sericea Biophysical Mapping

Assuming the environmental conditions (sunlight, temperature, moisture, etc) and leaf moisture of sericea were similar in a field, the major biophysical attributes that influenced sericea's spectral reflectance was its height and density that were closely related to green biomass. As a result, the variation of the maximal derivatives of sericea was primarily resulted from different height and ground cover of sericea for each pixel in these patches.

A loose logarithmic linear relationship could be observed in the scatterplots of maximal derivatives of sericea with its height and percent cover that were measured in the field. However, both relationships were weak and tended to saturate at the high end. This indicated that the variation of reflectance cannot be fully explained by a single biophysical attribute. For this reason, we defined a new variable, sericea "volume", to take both height and ground cover into consideration. Sericea "volume", referred to as *sericea_vol* in equations, was simply calculated as:

$$sericea_vol = H * fc \quad (2)$$

where H was sericea height (m) and fc was the fractional ground cover (×100%).

Since ground cover represented the area of sericea (m^2) in the projected unit ground area (m^2), sericea “volume” gave a sense of volumetric abundance of sericea in unit ground area (m^3/m^2). A quotation mark was added to this term because it was not a real volume definition (m^3) of the weed. By multiplying sericea height (H) and its horizontal ground cover (fc), Sericea “volume” captured the biophysical properties of sericea patches in a quasi 3-dimensional way, which could be used as an approximate measure of sericea invasiveness. A strong logarithmic linear relationship was observed in the scatterplot of maximal derivatives and sericea “volume” (Figure 3). With the curve fitting technique, sericea “volume” was estimated from maximal derivative (max_deriv):

$$Sericea_vol = -0.098 + 0.117 * \ln(max_deriv - 28.878) \quad (3)$$

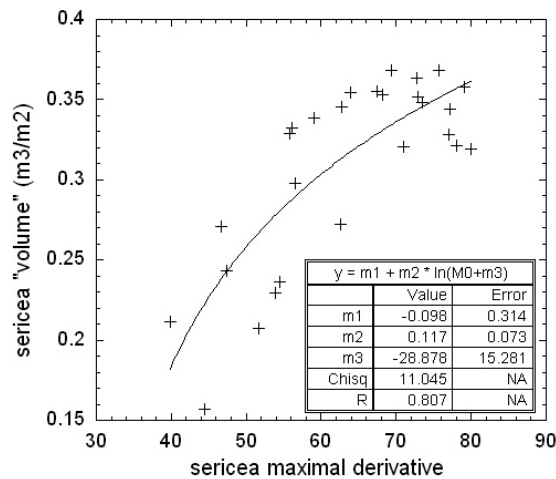


Figure 3. The scatterplot between maximal derivatives of sericea and the “volume”.

After binary sericea/non-sericea map was developed with the threshold method, sericea “volume” in each pixel of sericea patches could be calculated with Eq.3. The biophysical distribution of sericea was thus quantified to demonstrate its invasiveness in the study area.

RESULTS AND DISCUSSIONS

Using the threshold method described in previous section, sericea patches of various sizes were identified in the binary sericea map. The map obviously overestimated the problem of invasion because all sericea patches in the map were assumed homogeneously invading the field. It was observed during field surveys that sericea grew at various height and density. However, this variation cannot be observed in binary sericea map. Agreeing with field observations, the large, homogeneous field in the southeast corner of the map (out of the grass field) was dominated by sericea. The field was burned in 2005 in an attempt to eliminate sericea. Unfortunately, sericea grew back in 2006 more intensively while other species were killed (Dr. David Larson, Dept. of Forestry, University of Missouri, personal communication).

Sericea “volume” quantified biophysical variation of sericea patches in a range of 0.18-0.35 m^3 per unit ground area in the study field (Figure 4). It was found that small sericea patches often had low “volume”. In large patches, sericea “volume” in the center was high and it decreased toward the edges. The post-fire sericea regrowth in the southeast corner of the image had much higher volume than less-disturbed sericea patches inside the grass field. These characteristics agreed well with our field observations. This study demonstrated that hyperspectral imagery could effectively identify sericea patches in pasturelands and quantify the quasi 3D sizes of this weed in a “volume” map. As a result, it could provide more accurate information about the per-field state of sericea invasion.

This research agreed with past studies that narrowband remote sensing could provide significant improvement over broadband imagery in quantifying biophysical characteristics of vegetation (Shibayama and Akiyama 1991; Elvidge and Chen 1995; Thenkabail et al. 2000). Although large patches could be identified in typical broadband true-color aerial photos, biophysical variation of sericea in these patches could not be effectively quantified from these photos. Moreover, small patches, as well as the outer boundaries of large sericea patches, were often mixed with fescue because sericea was short and often mixed with fescue. These areas usually serve as seed patches along

which sericea expands outward year by year. The capability of narrowband imagery in identifying these areas provided important information in weed control and pastureland management programs.

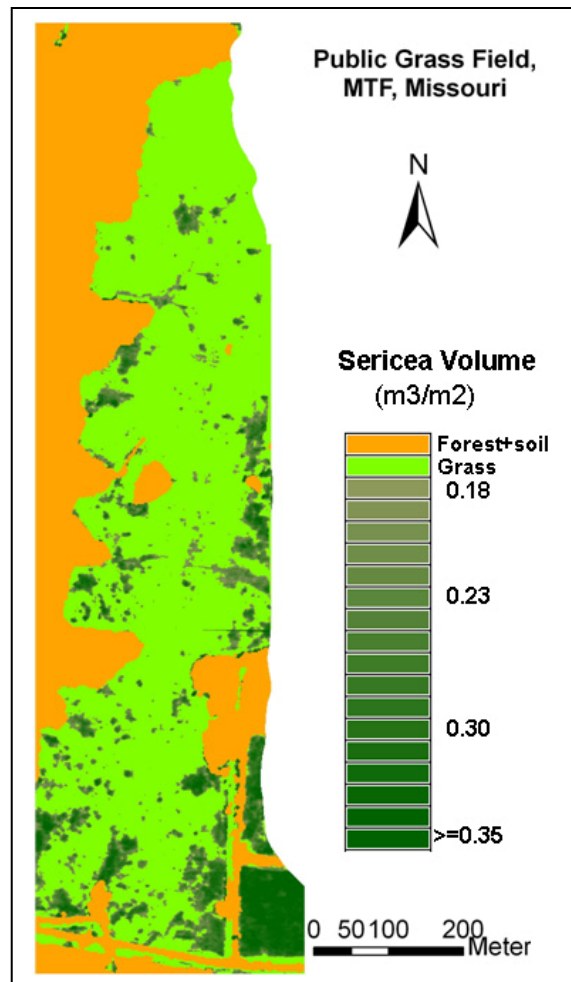


Figure 4. The sericea “volume” map in the public grass field.

CONCLUSION

Because of the similarity in color and height with fescue in pastures, sericea patches cannot be easily identified in typical true-color aerial photos. The subtle spectral difference between these two species could be detected in the narrow bands of hyperspectral images. In this study, a derivative analysis was applied to map sericea and its invasiveness in pasturelands using hyperspectral imagery. It was found in this study that, along the red edge, the maximal 1st-order derivative of Sericea was distinctly different from fescue in pasturelands in Mid-Missouri. The maximal derivatives of sericea was log-linearly related to sericea “volume” that could serve as a measure of sericea invasiveness in a quasi 3-dimensional way.

Sericea is gaining dominance in Missouri without much public awareness because the infected areas are often in less cultivated grasslands and remote pasturelands. By examining the effectiveness of hyperspectral imagery for detecting invasive weeds, this study will serve as a first step in alerting landowners and the general public about the seriousness of the problem.

ACKNOWLEDGEMENT

This research was supported by the Research Board Program at University of Missouri. Part of the results has been accepted to publish in the Environment Management journal. The authors would like to thank the Center for Advanced Land Management Information Techniques (CALMIT), University of Nebraska for hyperspectral image acquisition. We also highly appreciate the warmhearted help from Ms. Becky Erickson in the Regional Office of Missouri Department of Conservation and personnel in the Houston-Rolla-Cedar Creek Ranger District, Mark Twain National Forest for the assistance in field work.

REFERENCES

- Becker, B. L., D. P. Lusch, and J. Qi, 2005. Identifying optimal spectral bands from in situ measurements of Great Lakes coastal wetlands using second-derivative analysis, *Remote Sensing of Environment*, 97:238-248.
- Bové C., 2004. Missouri's silent thief, *Missouri Conservationist*:15-17, July.
- Brush L., 2001. Sericea lespedeza, *Today's Farmer*:14-15, May.
- Chen, Z. and P. J. Curran, 1992. Derivative reflectance spectroscopy to estimate suspended sediment concentration, *Remote Sensing of Environment*, 40:67-77.
- Demetriades-Shah, T. H., M. D. Steven, and J. A. Clark, 1990. High resolution derivatives spectra in remote sensing, *Remote Sensing of Environment*, 39:153-166.
- Dudley, D. M. and W. H. Fick, 2003. Effects of sericea lespedeza residues on selected tallgrass prairie grasses, *Transactions of the Kansas Academy of Science*, 106:166-170.
- Elvidge, C. D. and Z. Chen, 1995. Comparison of broad-band and narrow-band red and near-infrared vegetation indices, *Remote Sensing of Environment*, 54:38-48.
- ENVI, 1999. The Environment for Visualizing Images (ENVI): User's Guide, Research System Institute, USA.
- Filella J. P., P. Lloret, F. Munoz, and M. Vilajeliu, 1995. Reflectance assessment of mite effects on apple trees, *International Journal of Remote Sensing*, 16:2727-2733.
- Fitzgerald, G. J., S. J. Maas, and W. R. Detar, 2004. Spider Mite detection and canopy component mapping in cotton using hyperspectral imagery and spectral mixture analysis, *Precision Agriculture*, 5:275-289.
- Gamon, J. A., J. Peñuelas, and C. B. Field, 1992. A narrow waveband spectral index that tracks diurnal changes in photosynthetic efficiency, *Remote Sensing of Environment*, 41:35-44.
- Goetz, A. F. H., G. Vane, J. E. Solomon, and B. N. Rock, 1985. Imaging spectrometry for Earth remote sensing, *Science*, 211:1147-1153.
- Jensen, J. R., 2000. *Remote Sensing of the Environment: an Earth Resource Perspective*, Pearson Prentice Hall, Upper Saddle River, New Jersey, 544pp.
- Koger, C. H., D. R. Shaw, C. E. Watson, and K. N. Reddy, 2003. Detecting late-season weed infestations in Soybean, *Weed Technology*, 17:696-704.
- Peñuelas, J., J. A. Gamon, A. L. Fredeen, J. Merino and C. B. Field, 1994. Reflectance indices associated with physiological changes in nitrogen- and water-limited sunflower leaves, *Remote Sensing and Environment*, 48:135-146.
- Savitzky, A. and M. J. E. Golay, 1964. Smoothing and differentiating of data by simplified least squares procedures, *Analytical Chemistry*, 36:1627-1639.
- Shibayama, M. and T. Akiyama, 1991. Estimating grain yield of maturing rice canopies using high spectral resolution reflectance measurements, *Remote Sensing of Environment*, 36:45-53.
- Stitt, R. E., 1943. Variation in tannin content of clonal and open-pollinated lines of perennial lespedezas, *Agronomy Journal*, 38:1-5.
- Thenkabail, P. S., R. B. Smith and E. De Pauw, 2000. Hyperspectral vegetation indices and their relationships with agricultural crop characteristics, *Remote Sensing of Environment*, 71:158-182.
- Tsai, F. and W. Philpot, 1998. Derivative analysis of hyperspectral data, *Remote Sensing of Environment*, 66:41-51.
- Zhang, M., Z. Win, X. Liu and S.L. Ustin, 2003. Detection of stress in tomatoes induced by late blight disease in California, USA, using hyperspectral remote sensing, *International Journal of Applied Earth Observation and Geoinformation*, 4:295-310.